Accepted Manuscript

Core/shell emulsion micro- and nanocontainers for self-protecting water based coatings

Dmitry Grigoriev, Elena Shchukina, Aiym Tleuova, Saule Aidarova, Dmitry Shchukin

PII: S0257-8972(16)30002-0
DOI: doi: 10.1016/j.surfcoat.2016.01.002
Reference: SCT 20850

To appear in: *Surface & Coatings Technology*

Received date: 3 September 2015
Revised date: 31 December 2015
Accepted date: 2 January 2016

Please cite this article as: Dmitry Grigoriev, Elena Shchukina, Aiym Tleuova, Saule Aidarova, Dmitry Shchukin, Core/shell emulsion micro- and nanocontainers for self-protecting water based coatings, *Surface & Coatings Technology* (2016), doi: 10.1016/j.surfcoat.2016.01.002

Core/shell emulsion micro- and nanocontainers for self-protecting water based coatings

Dmitry Grigoriev[a]*, Elena Shchukina[b], Aiym Tleuova[c], Saule Aidarova[c] and Dmitry Shchukin[b]

[a]*Max Planck Institute of Colloids and Interfaces, Am Muehlenberg, 14476 Potsdam, Germany*

[b]*University of Liverpool, Crown Street, Liverpool L69 7ZD, United Kingdom*

[c]*International Postgraduate Institute "Excellence PolyTech" of Kazakh National Technical University, Satpaev Street 22, 050013 Almaty, Kazakhstan*

Keywords: coatings, corrosion protection, inhibitor, encapsulation, emulsion route, morphology

Abstract

Gradual substitution of anticorrosive coating formulations revealing hazardous effects on the environment by eco-friendly ones is nowadays an ongoing trend in the coating industry. The main pathways here are the exchange of environmentally toxic anticorrosive pigments by less toxic components and reduction of content of volatile organic compounds used as solvents and thinners by increasing usage of waterborne coating formulations. The side effect is the decrease of the total corrosion protection performance of new coatings. A possible solution of this problem could be incorporation of tiny polymeric micro- and nanocontainers loaded with "green" corrosion inhibitors into protective coatings. In this work, the detailed description of containers syntheses via emulsion route and their comprehensive characterization are followed by numerous examples of containers successful application in the novel anticorrosive coatings showing the significant improvement of corrosion protection performance.

*Corresponding author. Tel. +49-3315679257; email: dmitry.grigoriev@mpikg.mpg.de

1. Introduction

Development of environmentally benign coating formulations is nowadays one of the most pronounced trends in the coating industry and, in particular, in the field of corrosion protection coatings. Driven by steadily rising governmental requirements to ecological standards, the main efforts here are focused simultaneously on two very ambitious goals: strong reduction or complete elimination of hazardous materials in the coatings and maintaining or even improving their protective performance. The attainment of the first of these aims is strongly associated with exclusion of environmentally harmful anticorrosive pigments (ACPs) like chromates etc. from the coating compositions or substitution of them with the same or lower amounts of less hazardous ingredients. There is, however, a second group of environmentally dangerous substances widely used in contemporary coating formulations, which is comprised of various volatile organic compounds, so-called VOC that can ingress in the environment during production, application or curing of the solvent based coating formulations. Reduction of VOC emissions is therefore the other big problem that needs to be solved on way to more ecofriendly coatings and draws governmental attention on both national [1] and international [2] level.

Waterborne polymeric coating formulations like formulations on the basis of styrene/acrylic polymer/copolymer emulsions/dispersions or diverse formulations based on modified alkyd resin emulsions are currently one of the most rapidly growing groups of protective and anticorrosive coatings [3-6] aimed at lowering the VOC emissions. A relatively low level of the corrosion protection [7-9] especially for the compositions without special protective ingredients is however their main drawback. The ability of these coatings to be a good barrier against the permeation of water, oxygen, and other corrosive species is quite weak due to various factors such as residual hydrophilic components and low cross-linking degree often related to purely physical curing mechanism. Because of this peculiarity, significant amounts

of corrosion protection additives, mainly – ACPs – are established today to be an indispensable part of these formulations intended for the efficient metal protection. Their content can in some cases attain up to 15 wt% of the total liquid weight to ensure the satisfactory protective performance. Further enhancement of anticorrosive performance in the same fashion is hardly achievable: Increase of pigment concentration can worse the barrier properties of the coating and will aggravate environmental stress connected with the use of these coatings in spite of lower pigment toxicity.

In order to break this vicious circle, the novel solution based on the inhibitor filled micro- and nanocontainers embedded in the coating matrix was recently proposed [10, 11]. In the work at hand the principles of this new approach were applied to several waterborne VOC-low coatings using selected types of abovementioned containers prepared via emulsion route. Environmentally benign adsorption inhibitors were loaded into containers to ensure the "green" and sustained protective effect [10-13]. Apart from the comprehensive characterization of synthesized containers, the anticorrosive performance of coatings with embedded containers was compared with the corresponding properties of the conventional coatings.

2. Materials and methods

2.1. Chemicals

Poly[(phenyl isocyanate)-co-formaldehyde] (isocyanate prepolymer, average number of isocyanate groups per molecule ~3.2, MW~400), ethylenediamine (EDA), tetraethylenepentamine (TEPA), diethylenetriamine (DETA), carbamide, poly(vinyl alcohol) (PVA, MW~9,000-10,000, 80% hydrolyzed), diethyl phthalate (DEPh), hexadecane, 2-methyltetrahydrofuran (MeTHF), 8-hydroxyquinoline (8-HQ), 2-methylbenzothiazol (MeBT),

1,2,3-benzotriazole (BTA), trimethylolpropane triglycidyl ether, tris(4-hydroxyphenyl)methane triglycidyl ether, tetrabutylphosphonium bromide of reagent grade (at least 98 wt% purity or higher) were obtained from Sigma-Aldrich Corporation, Germany and used as received. Ultrapure MilliQ Plus 185 water (resistivity = 18.2 MΩ·cm) was used in all experiments.

2.2 Methods

2.2.1 Preparation of polyurea (PUa) micro- and nanocontainers

PUa micro- and nanocontainers loaded with corrosion inhibitors 8-HQ and MeBT were prepared via emulsion route (starting from oil-in-water "O/W" emulsions) by interfacial polyaddition. This is a well-established technique for the preparation of various polymeric capsules and particles with sizes ranging from some hundreds of nanometers to some micrometers. Typically, O/W emulsion is prepared in the first step in which at least one of monomeric or oligomeric reactants is dissolved in the emulsion droplets. An active agent (in our particular case – corrosion inhibitor) should also be soluble predominantly in the dispersed phase to be finally encapsulated. Very often, one uses an appropriate auxiliary co-solvent [10, 11] with good solvency for both these components to circumvent their mutual immiscibility – oily phase should be homogeneous prior to the emulsification (Fig.1A). Continuous phase of this initial emulsion contains as a rule either surfactant or dispersing agent ensuring its stability at least until a second step of containers synthesis. In the second step, either the initial emulsion is added to the miscible solution containing the second (monomeric) reactant or this solution is added to the initial emulsion (Fig.1A). The reactants come into contact on the boundary between two liquid phases and interfacial polyaddition occurs. Both reactants possess initially different polarities and are mainly soluble in one

particular phase limiting their sufficient interpenetration in the coexisting phases and excluding premature reaction between them. In ideal case, reactants have to be kept phase-separated all the time when reaction goes on and meet each other only at the interface of

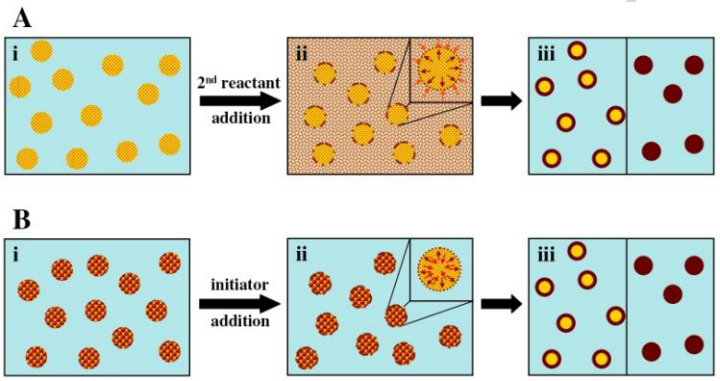

Figure 1. A: i – Preparation of initial emulsion with the dispersed phase containing corrosion inhibitor and first reactant participating in the interfacial polyaddition reaction, emulsion stabilizer/surfactant is dissolved in the dispersion medium; ii – Addition of bulk-soluble second reactant for the interfacial polyaddition in the pre-formed emulsion and start of polyaddition reaction. Inset – interfacial polyaddition process on the boundary of emulsion droplets; iii – Completion of micro- or nanocontainers formation with core/shell or compact morphology. B: i – Preparation of an initial emulsion with the dispersed phase containing corrosion inhibitor and all reactants needed for the in-situ polyaddition, emulsion stabilizer/surfactant is dissolved in the dispersion medium; ii – Addition of bulk-soluble initiator for the polyaddition reaction in the pre-formed emulsion and start of in-situ polyaddition. Inset – in-situ polyaddition reaction in the bulk of each emulsion droplet; iii – as in A iii.

emulsion droplets. If the polymerization products are soluble neither in the droplets of the dispersed phase nor in the medium around them, the core/shell morphology of containers will be achieved. More frequently however, the polyaddition products are soluble or swellable in the composition of dispersed phase and particles with the compact morphology occur.

The principal chemical reaction leading to the formation of PUa cross-linked network at the liquid-liquid interface can be presented by to the following reaction scheme:

$$nOCN-R-NCO+nH_2N-R'-NH_2 \rightarrow \left[-OC-NH-R-NH-CO-NH-R'-NH-\right]_n \quad (1)$$

The preparation route similar to one presented recently [12, 13] was used for the synthesis of PUa containers. Typically, the abovementioned isocyanate prepolymer was mixed with the liquid corrosion inhibitor MeBT at ratio 3:7 (w/w) and resulting oil phase was emulsified in 10 times higher amount of aqueous solution (2.5 wt%) of PVA as emulsion stabilizer. For this purpose, Ultra-Turrax high-speed homogenizer (IKA Werke, Germany) was utilized (3 minutes, 17000 rpm). The initial O/W emulsion was then mixed with the same amount of 25

wt% aqueous solution of EDA and TEPA (1:3, w/w) by the dropwise addition of the latter under continuous stirring. As alternative, an aqueous mixed solution of carbamide and TEPA (5:1, w/w) with 2.5 times lower concentration can be used. After addition was finished, the mixture was stirred for another 15 minutes and then left to stay overnight without stirring until the polyaddition reaction is completed. Finally, the ready containers were washed several times with MilliQ water and dried under mild conditions.

For the preparation of containers loaded with the corrosion inhibitor 8HQ, a slightly modified synthesis technique was chosen. Here, the main difference was caused by the utilization of several auxiliary solvents needed for the good miscibility of 8HQ and prepolymer. Typically, either DEPh or MeTHF were used for this purpose. The first solvent can dissolve up to 18 wt% of inhibitor and is practically immiscible with water or aqueous dispersion media. MeTHF is slightly soluble in water but its solvency for 8HQ exceeds the level of 35 wt%. The utilization of diverse auxiliary solvents can be therefore used for adjusting the desired concentration of inhibitor in the containers. Another slight difference at the synthesis of 8HQ loaded PUa containers consisted in the use of tiny amounts of hexadecane as hydrophobe in the oily phase prior to the preparation of initial emulsions. This additive was needed to decrease the total polarity of oil because of higher polarities of 8HQ and MeTHF comparing with MeBT (the more detailed preparation procedure for the PUa containers loaded with 8HQ is given in the section S2 of the Supporting Information). As a result, the more monodisperse containers with smaller size were obtained.

2.2.2 Preparation of polyepoxy (PE) micro- and nanocontainers

The polyepoxy containers filled with the corrosion inhibitors BTA and MeBT were prepared by in-situ polyaddition method. Realization of this technique is also related to emulsion route for containers fabrication presuming however, that all reactants needed for the synthesis are

contained in the oily phase already from the beginning. After emulsification, the droplets of the initial emulsion play simultaneously the two-fold role of reservoirs for reactants and inhibitors as well as of liquid colloidal reactors and are in the ”frozen”, only kinetically-stable state (Fig.1B). To start the reaction in the droplets of W/O emulsion with desired properties, one needs to apply either chemical (initiator substance, catalyst) or physical (T, UV-light etc.) triggers (Fig.1B). Being switched on in this fashion, the in-situ polyaddition process runs until the real equilibrium is achieved upon reaction completion. Similarly to the case of interfacial polyaddition, the containers with compact, core/shell or even multicompartment [11] morphology can be synthesized depending on the solubility/swellability of the growing polymers in the inner material of droplets. On the other hand, initial kinetically-stabilized state of emulsion droplets may be utilized for the controllable initiation of the polyaddition from outer phase simultaneously at the entire droplet interface. If this reaction is fast enough, the cross-linking degree and molecular weight of this forming “interfacial” polymer can lead to the kinetically stable core/shell structures that can be obtained in spite of good solubility of smaller oligomers [14].

The principal chemical reaction responsible for the polyepoxy linkage formation can be written as follows:

$$n\mathrm{H_2C}\!-\!\underset{\diagdown\,\diagup}{\mathrm{CH}}\!-\mathrm{R''}\!-\!\underset{\diagdown\,\diagup}{\mathrm{CH}}\!-\mathrm{CH_2} + n\mathrm{H_2N}\!-\mathrm{R'}\!-\mathrm{NH_2} \rightarrow$$
$$\rightarrow n\mathrm{H_2N}\!-\mathrm{R'NH}\!-\mathrm{CH_2CH(OH)}\!-\mathrm{R''}\!-\mathrm{CH(OH)CH_2}\!-\mathrm{NHR'}\!-\mathrm{NH_2} \qquad (2)$$

PE containers were prepared according to the synthetic algorithm described in details in [10]. In brief, the following subsequent steps were conducted: First, the shell-forming epoxy group-bearing monomers trimethylolpropane triglycidyl ether (aliphatic) and tris(4-hydroxyphenyl)methane triglycidyl ether (aromatic) were mixed together at a ratio 1:1 (w/w). Then, the corrosion inhibitor MeBT was added to the initial monomer mixture in the amount of 20 wt% to its total weight. In the second step of preparation, this oil phase of the future emulsion was mixed with polyfunctional monomer serving as a second reactant in the

polyaddition reaction – DETA. Typically, DETA was taken in the amount slightly exceeding the stoichiometric equivalence with epoxy groups. Finally, the oil phase was emulsified in the 2 wt% aqueous PVA solution by means of high speed rotor-stator homogenizer (5 minutes, 16000 rpm) and in-situ polyaddition process was activated by addition of small amount of polymerization catalyst tetrabutylphosphonium bromide. The polymer formation was completed overnight under room temperature and moderate stirring. For the synthesis of BTA loaded PE containers, other mixing sequence of the components was applied. In the first step, both epoxy monomers were mixed together (1:1, w/w) and with 1 wt% hexadecane (to the total mass of them) under heating at 80° C in order to decrease the system viscosity and ensure better homogeneity. Then, a 19 wt% solution of BTA in DETA was prepared also using similar mixing conditions. After both these mixtures were cooled down they were mixed together at the ratio 1:1 forming the oil phase of the future emulsion. Emulsification process was conducted directly in the aqueous 0.25 wt% PVA solution containing 1.2 wt% of tetrabutylphosphonium bromide. The resulting O/W emulsion was very intensively stirred (high speed rotor-stator homogenizer, 6 minutes, 20000 to 24000 rpm) and then left to mature under weak stirring over one day. Finally, ready-made containers were separated by filtration, washed two times with MilliQ water and dried under mild conditions.

2.2.3 Preparation of coating formulations with micro- and nanocontainers

Conventional waterborne styrene acrylic copolymer emulsions, air drying fatty acid modified or short oil modified alkyd resin emulsions were used in this work as initial systems for the preparation of novel nano- and microcontainers based anticorrosive coating formulations. Also, abovementioned conventional coatings were utilized in comparative tests of corrosion protection performance as references. Containers containing coating formulations were fabricated by the complete exclusion of the ACPs fraction composed of inorganic and organic

zinc based compounds from conventional formulations immediately on the step of their preparation (dummy coatings) and by the subsequent addition of a certain amount of inhibitor loaded containers to this ACP-free dummy mixture. Typically, container amounts from 2.5 wt% to 5 wt% in relation to the total dry weight of the cured coating were added. As a rule, these amounts of container based additives were essentially lower than amounts of excluded ACPs. Total contents of ACPs were ranged between 7.5 wt% and 10.5 wt% for the conventional coating formulations based on modified alkyd resin emulsions and styrene acrylic copolymer emulsions, respectively. These concentrations of ACPs equate to the fractions of anticorrosive pigments 25 wt% and 30 wt% with respect to the total pigment content and do not exceed the corresponding critical pigment concentrations. Neutral fillers like barium sulfate or magnesium silicate were added to the dummy formulation to close this pigment gap and to maintain the total pigment concentration on the level common for the conventional coating formulations. Incorporation of the corresponding amount of containers to the dummy coating formulation was conducted as follows: a chosen amount of containers was added to the formulation by several subsequent steps under moderate stirring with dissolver (about 2000 rpm) until the entire mixture became well-homogenized. Viscosity of the resulting mixture was controlled by using of a flow cup with 4 mm orifice diameter. In case, the time in which a defined volume of containers modified coating formulation flowed out through the orifice was too high the viscosity of the mixture was reduced to the regular level by addition of necessary water amount to ensure a problem-free application by means of a spray gun.

2.2.4 Preparation of test panels for the salt spray testing

Commercially available steel test panels GARDOBOND OC (Chemetall, Germany) or Q-Panel R-35 (Q-Lab, USA) with dimensions (TxWxL) of 3x105x190 mm or 0.8x76x127 mm,

respectively, were used for the salt spray tests. These panels were cleaned and then coated by the corresponding coating formulation using the spray gun set-up with the nozzle diameter 1.4÷1.6 mm and processing pressure 4 to 5 bars. After application, the freshly coated panels were left for room temperature curing process which lasted 7 day for styrene acrylic copolymer emulsions and 14 days in case of alkyd resin emulsions. Alternatively, panels coated by styrene acrylic copolymer emulsions can be subjected to accelerated curing procedure at 50-60° C for 12 hours. The dry film thicknesses (DFT) of 55 ± 6 µm and 80 ± 9 µm were measured for the testing panels coated with formulations based on both types of modified alkyd resin emulsions and styrene acrylic copolymer emulsions, respectively. The coating thickness was determined by means of a coating thickness gauge, Surfix® Pro S, from Phynix GmbH, Germany. The subsequent steps of the panels preparation process are given schematically in the Figure 2. Before testing in the salt spray chamber, the cured panels were handled as follows: the cut edges and back surface were protected using a transparent Scotch tape or, in some cases, they were sealed by dip coating with the molten paraffin. Then, in the middle part of each panel a vertical scribe with the length of 70 ± 5 mm (Q-Panels) or 100 ± 5 mm (GARDOBOND OC panels) and width 1 mm was made using the scribing tool according to Sikkens.

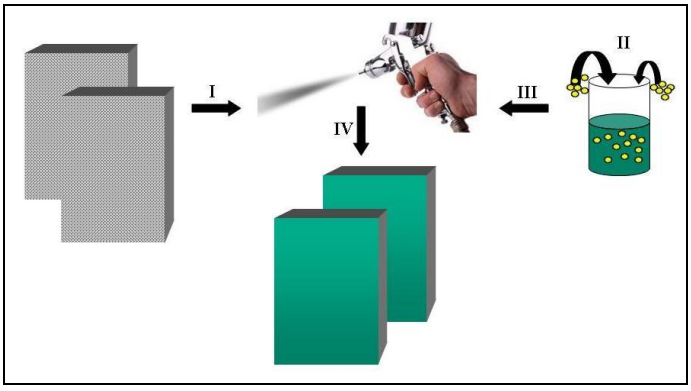

Figure 2. Schematic illustration of the test panels preparation process: I – degreasing; II – incorporation of containers in an appropriate coating formulation; III – application by spraying; IV – curing.

2.2.5 Methods for characterization of containers and their performance in the coatings

Scanning electron microscopy (SEM). SEM measurements were carried out using a Gemini Leo 1550 instrument at an operation voltage of 3 keV. The samples were prepared by placing containers aqueous suspension onto a glass substrate, drying and subsequent gold sputtering.

TSEM measurements. An FE-SEM of type Supra 40 (Zeiss, Oberkochen, Germany) was employed, equipped with an in-lens detector. The important information on the sample structure beyond its surface (in-depth scanning) was obtained by transmission mode in SEM (TSEM). The STEM detector placed immediately under the thin sample was utilized for acquiring TSEM images in this mode. In the present study, a commercial transmission setup has been used (single-unit transmission setup) which functioned as a sample holder that guided the transmitted electrons onto an electron multiplier and then to the conventional Everhart–Thornley detector.

Fourier Transform Infrared (FTIR) Spectroscopy. FTIR spectra were recorded at room temperature in KBr pellets using a Bruker Hyperion 2000 IR spectrometer equipped with a 158 IR objective. The pellets were prepared by mixing the dried containers in powder form and potassium bromide and subsequent utilization of manual pellet press (Specac, Orpington, UK). Resulting pellets were then mounted on a QuickLock base plate. Spectra were acquired in the transmission mode between 400 and 4000 cm^{-1} with 2 cm^{-1} resolution by means of a DTGS detector.

Size distribution and Zeta-Potential measurements. These parameters were measured by dynamic light scattering (DLS) using the Zeta Sizer Nano (Malvern Instruments, UK). The aqueous suspensions of containers (MilliQ water) with appropriate concentrations were subjected to these measurements at 25° C. The size distribution was measured in polystyrene cuvettes with 1.5 mL volume. The measurements of the Zeta-potential were conducted in disposable capillary cuvettes with volume of 1 mL. The water viscosity and refraction index were set to those of dispersion medium. Size distribution measurements were done in

backscattering mode at a detector position of 173°. The scattering data were analyzed using the CONTIN algorithm. Size distribution data were averaged over three measurements with at least 15 runs in each. The Zeta-potential values were calculated from the electrophoretical mobility automatically by the instrument. Each value was found as an average from three sequential measurements.

UV-VIS Spectroscopy. UV-VIS spectra were recorded at room temperature in a 10 mm quartz cuvette by means of a UV-VIS spectrometer Varian Cary 50 Conc (Varian, USA) in the wavelength range from 200 to 800 nm and 0.5 nm resolution. The wavelengths for the quantitative determination of inhibitors during the release experiment in aqueous media were 218 nm, 239 nm and 256 nm for MeBT, 8HQ and BTA, respectively.

TGA measurements. Thermogravimetric analysis was performed by means of a Netzsch TG 209 F1 setup with a heating rate 10 K/min under N_2 atmosphere.

Release in aqueous media.

The release kinetics of inhibitors enclosed in different types of containers was carried out in aqueous media with various pH values mimicking the local pH changes which can be caused by the corrosion onset. The glass beaker with the total volume of 1000 ml was filled with aqueous medium with the corresponding pH value set by small amounts of HCl or NaOH. 10 grams of containers under investigation were dispersed in this medium and left under moderate continuous stirring (300 rpm). After defined time intervals, the suspensions aliquots of 2 ml were withdrawn in triplicate and replaced with the same aqueous solution. The collected samples were centrifuged at 13000 rpm for 10 minutes in order to separate the supernatant from the dispersed containers. The obtained particle-free supernatant was then analyzed by UV-VIS spectroscopy taking into account the signal intensities at wavelengths listed in the section 2.2.5. The intensity values were used for the evaluation of inhibitor concentrations in the release medium and to the subsequent calculation of its release ratio corresponding to the time point of sample withdrawal.

Neutral salt spray test (NSS test).

Coated steel panels were subjected to a neutral salt spray test (NSS test) according to ISO 9227 (ASTM B117) [15]. For this purpose, the scribed panels were placed on the special racks in the salt spray chamber CC450XP (Ascott, UK) with the total inner volume of 450 L and conditions leading to the accelerated onset of corrosion: 100% rh, T = 35° C, continuous spraying a 5 wt% aqueous NaCl solution. The duration of NSS test was set in accordance with the expected corrosion resistance of the coating to be tested and lasted from 140 to 1000 hours.

3. Results and discussion

3.1 Characterization of containers

Fourier Transform Infrared Spectroscopy (FTIR).

FTIR measurements were used as a tool for qualitative checking the completion of polyaddition reaction at the containers formation made of PUa. Very weak bond intensity at 2276 cm^{-1} specific for the isocyanate group indicates almost complete transformation of NCO groups due to reaction with amines and urea monomers (Figure 3).

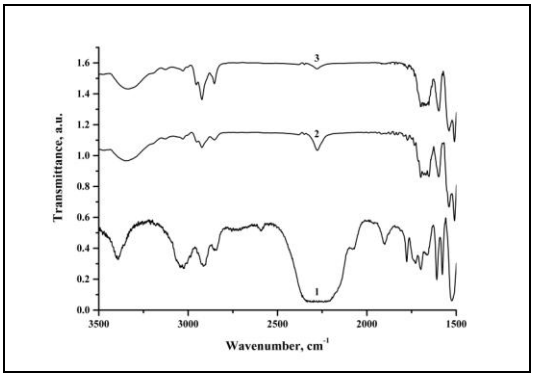

Figure 3. Gradual increase of the isocyanate conversion degree in the course of PUa containers formation: 1 – initial "oil" phase containing unreacted isocyanate prepolymers; 2 – premature containers after first 30 minutes of synthesis; 3 – ready containers.

Unfortunately, this method for the control of the conversion completion is hardly applicable to the synthesis of PE containers because the most distinctive bonds characteristic for epoxy and amino groups participating in this reaction are located in the near infrared wavelengths range [16 and references therein]. The completion of well cross-linked polyepoxy resin during containers synthesis was followed by TGA measurements.

Zeta-Potential and Size distribution.

Indirectly, the high conversion degree of isocyanate groups during the synthesis of PUa containers is confirmed by the results of Zeta-potential measurements. The corresponding values are in the range between +35 and +45 mV because of positive charge of amide surface groups occurring in the course of this polyaddition reaction. As one example, five subsequent Zeta-potential measurements data sets for PUa containers loaded with inhibitor 8HQ are plotted in the Figure 4a. Similarly, secondary and tertiary amino groups forming at the synthesis of PE containers cause the positive charge of their surface (Fig. 4b) especially

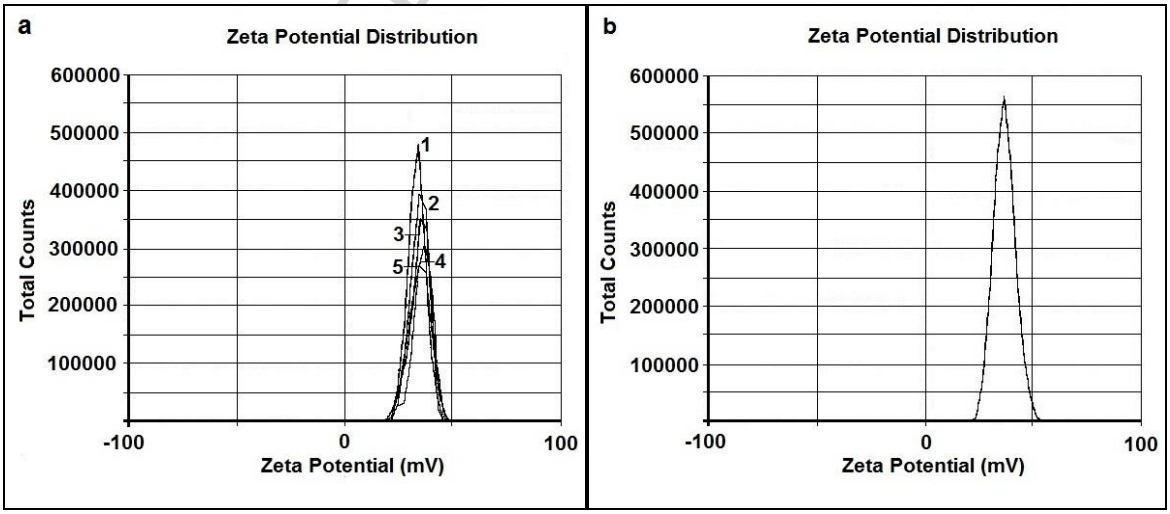

Figure 4. a – Results of several subsequent Zeta-potential measurements obtained at pH 7 for aqueous suspension of PUa containers loaded with the corrosion inhibitor 8HQ; b – Zeta-potential measured for aqueous suspension of MeBT filled PE containers at pH = 6.7.

taking into account a slight excess of amino-monomers used in this synthesis as was mentioned above in the section 2.2.2.

Micro- and nanocontainers size distributions obtained by DLS (zeta average) are presented in Figure 5 a-e. Although almost all size distributions are shown as monomodal curves (except

the curve in the Figure 5b, where two merged peaks are observed) the corresponding polydispersity indices (PDI) are quite high and within a range between 0.2 and 0.5.

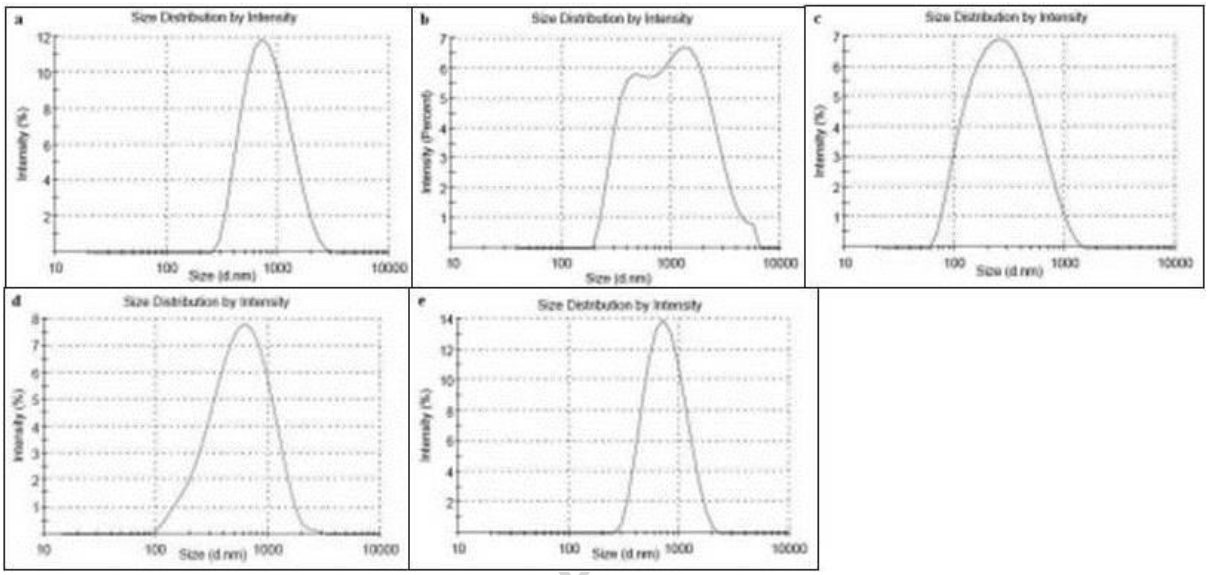

Figure 5. Size distributions of PUa and PE containers (zeta average) determined by DLS for their aqueous suspension in neutral pH range: a – PUa containers loaded with the corrosion inhibitor 8HQ using DEPh as an auxiliary solvent in the step of the initial emulsion preparation; b – as in a. but with MeTHF as an auxiliary solvent; c – PUa containers loaded with the liquid corrosion inhibitor MeBT; d – PE containers loaded with the corrosion inhibitor BTA; e – PE containers loaded with the liquid corrosion inhibitor MeBT.

These data are in a good accordance with the visual observations of corresponding containers made by SEM and TSEM (Figures 6a-6f) and presented in the paragraph "Morphology" below. Usually, a wide size distribution of particles obtained via emulsion route by polymerization is caused by a high-speed rotor–stator homogenizer utilized for the preparation of an initial emulsion [17]. Application of other comminution methods for this purpose (like high pressure homogenizer or ultrasound) can provide an essentially narrower and a really monomodal size distribution of droplet in an initial emulsion. On the other hand, intensive energy dissipation processes accompanying these methods may lead upon usage of quite reactive monomers or prepolymers to the numerous premature side reactions like, for example, water sonolysis, radical formation and other sonochemically induced phenomena in the case of ultrasound.

Nevertheless, the observed average container sizes do not exceed in spite of relatively broad distributions the upper limit of some micrometers. This size cutoff can ensure the full and

homogeneous incorporation of containers in the matrices of coatings which possess typically thickness of some tens of micrometers and allows therefore avoiding the coatings integrity deterioration even in the possible cases of the weak containers agglomeration like doublets or triplets formation.

Morphology (SEM and TSEM).

Morphology of resulting nano- and microcontainers is dependent on the polarities differences of the initial components and polymeric reaction products and can be quantitatively described in framework of Hansen solubility approach [18]. In the paper at hand, the interrelation between mutual solubilities (miscibilities) of containers components and their morphologies is discussed on the qualitative level. Quantitative considerations of this topic are beyond the scope of this paper and can be found in several recent publications [13, 14, 19].

PUa containers loaded with 8HQ by means of DEPh have spherical shapes with surface concavities and folds (Fig. 6a). The surface topography allows the suggestion that these

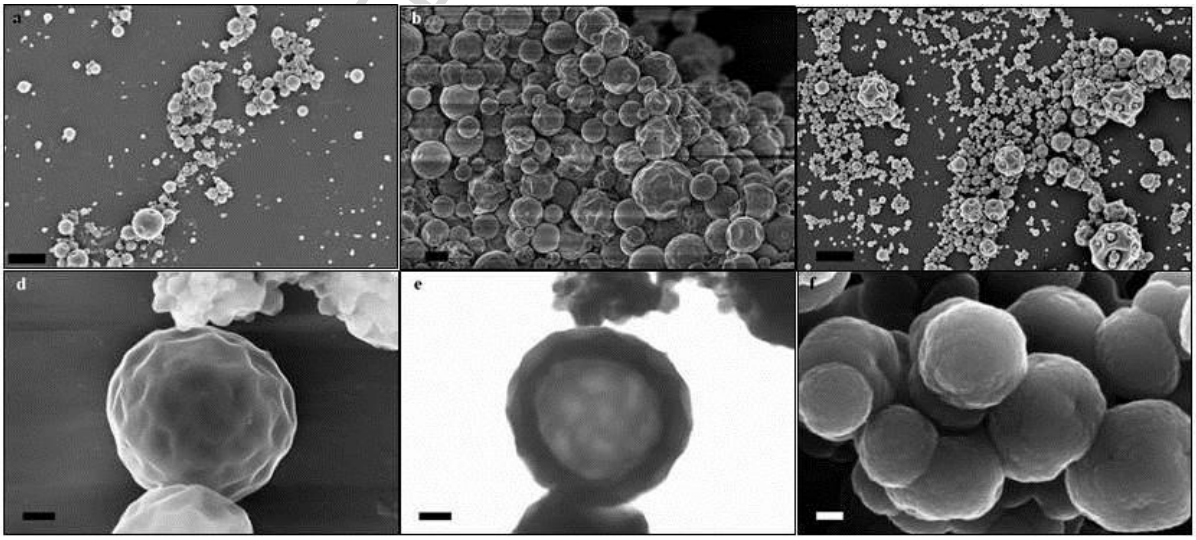

Figure 6. SEM and TSEM observations of inhibitor loaded PUa and PE containers: a – PUa containers loaded with the corrosion inhibitor 8HQ using DEPh as an auxiliary solvent; b – PUa containers loaded with the corrosion inhibitor 8HQ using MeTHF as an auxiliary solvent; c – PUa containers loaded with the liquid corrosion inhibitor MeBT; d and e – PE containers loaded with the corrosion inhibitor BTA in SEM and TSEM mode, respectively; f – PE containers loaded with the liquid corrosion inhibitor MeBT. Scale bars correspond to 2 µm, 1µm, 300 nm and 100 nm for pictures a and b; c; d and e; and f, respectively.

containers at least on the previous stage of their ripening had a core/shell morphology and could have the same morphology also in the mature state. On the other hand, we showed in

our previous work that the particles obtained by the interfacial polymerization of the oil phase composed of only isocyanate prepolymer and DEPh have a compact morphology [14]. Taking into account that the polarity of inhibitor 8HQ [20, 21] added to the containers discussed here is higher than the polarity of the pure solvent DEPh [22], one can assume the higher total polarity of the oil phase and, therefore, the most probably compact morphology of containers. PUa containers loaded with 8HQ via MeTHF route with essentially higher polarity comparing with DEPh should also have the same compact morphology in spite of numerous concavities on the surface (Fig. 6b) and even some crumpled containers clearly observable on this SEM photograph. The same considerations are also valid for the morphology of PUa capsules loaded with liquid corrosion inhibitor MeBT (Fig. 6c) and were reported in more details elsewhere [13].

The morphologies of the PE containers were analyzed in the same manner. Figure 6d represents the comparison of SEM and TSEM pictures obtained for BTA loaded PE containers. On the first glance, these containers have almost the same outer appearance (Figs. 6d and 6e) as PUa containers described above and may also have the compact morphology. On the other hand, the TSEM picture clearly shows that some of these containers have well-expressed core/shell morphology whereas other neighboring ones are compact. This polymorphism of PE containers could only be explained by kinetic factors playing an important role during the containers formation as mentioned above (see section 2.2.2). According to general considerations, the polarity of resulting cross-linked epoxy polymer should not differ significantly from polarity of PE containers load made of BTA and their most probable morphology is expected to be compact one. Thus, the presence of partially observed containers with the core/shell morphology is a clear evidence of kinetically caused demixing when the quickly increased degree of cross-linking of growing polymer hampers its dissolution in the core material. Finally, the PE containers loaded with the liquid corrosion inhibitor MeBT demonstrate (Fig. 6f) a well-distinguishable compact morphology which

could be related to low polarity difference between PE polymer and MeBT and thus to the good solvency of latter for the forming polymer. The abovementioned morphology of containers remains not disturbed also after their incorporation in the matrix of the cured coating. Example of the intact PUa micro- and nanocontainers with the corrosion inhibitor MeBT embedded in the of coating on the basis of the waterborne styrene acrylic copolymer emulsion and their homogeneous distribution in the coating matrix are shown in the Figure S1 in section S1 of the Supporting Information (SI).

TGA.

Relative amounts of inhibitors really loaded in the containers were evaluated by means of TGA. Figure 7a shows the results of comparative TGA measurements for the PUa containers loaded with corrosion inhibitor 8HQ using MeTHF as an auxiliary solvent. For the 8HQ in the free state practically whole sample is diminished as the temperature reach the level of about 200° C because of quite volatile character of this substance. In the enclosed state (in containers) the evaporation rate is strongly restricted at relatively low temperatures and can only attain a significant rate at the temperatures close to the boiling point of 8HQ (267 °C at atmospheric pressure). The cross-section of the vertical straight line representing this temperature and the TGA curve for the 8HQ loaded PUa containers showed about 11 wt% of the encapsulated inhibitor in the discussed case. This value is essentially lower than the

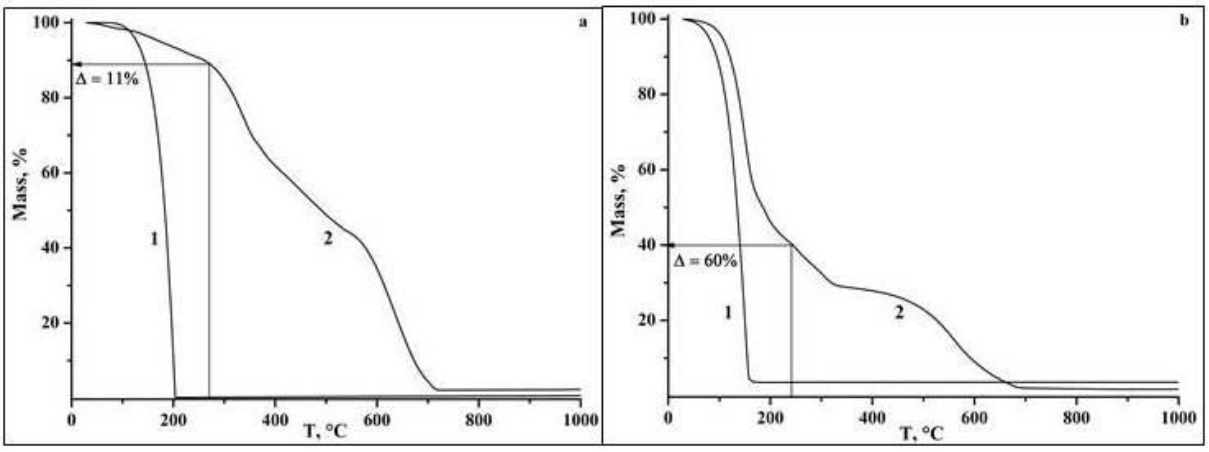

Figure 7. a – TGA curve of PUa containers loaded with the corrosion inhibitor 8HQ (2) compared with the TGA of the pure substance (1); b – TGA curve of PUa containers loaded with the liquid corrosion inhibitor MeBT (2)

compared with the TGA of the pure substance (1). Vertical straight lines correspond to the boiling points of pure 8HQ and MeBT.

theoretical one which could be calculated on the basis of initial amount of oil phase components and concentration of 8HQ in MeTHF solution used for the containers preparation. On the other hand, a certain loss of 8HQ from the oil phase should be taken into account especially because of slight solubility of MeTHF in the aqueous dispersion medium, its transfer towards this medium on the emulsification step and resulting increase of 8HQ solubility in the aqueous phase. TGA curve for the PUa containers loaded with the liquid corrosion inhibitor versus the corresponding curve for the pure substance is given in the Figure 7b. Here, because of essentially lower loss of sparingly soluble MeBT in the aqueous dispersion medium and absence of any auxiliary solvents in the system, the quantity of residual inhibitor enclosed in the containers is significantly higher and amounts at 60 wt% [13]. Again, the unrestricted evaporation of the same substance in the pure state is finished already far below 200° C however the boiling point of MeBT at atmospheric pressure is 238° C.

3.2 Release of encapsulated inhibitors in model aqueous media

Release kinetics from containers is presented in Figure 8 by two examples comparing the release of two different inhibitors – 8HQ and MeBT – from two chemically different types of containers matrices: PE and PUa. Whereas the release of 8HQ from PUa containers demonstrated a clear tendency to be dependent on the pH value of the release medium outside (Fig. 8a), the data collected for the release kinetics of MeBT from PE containers seemed to be almost insensitive (Fig. 8b) to pH changes.

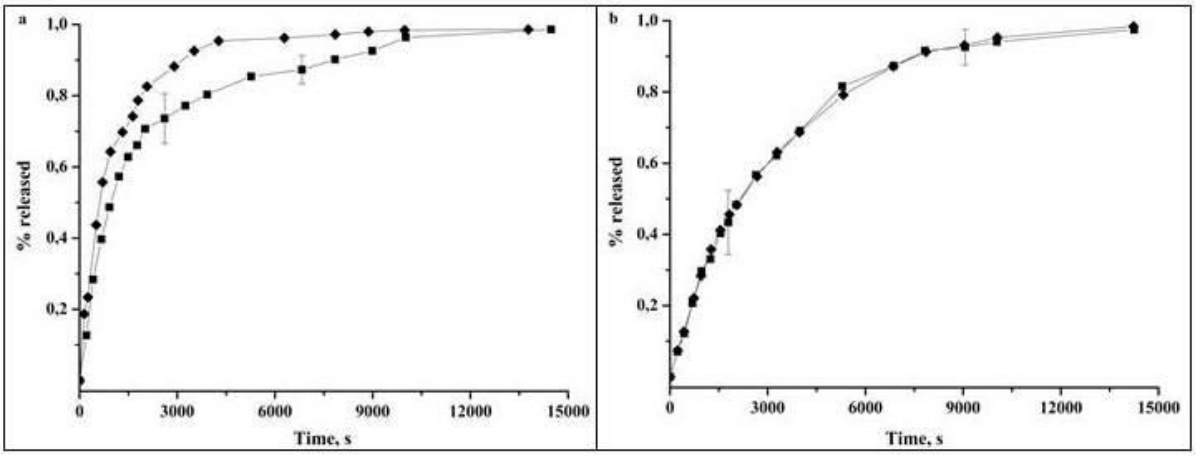

Figure 8. a – release kinetics of 8HQ enclosed in PUa containers: squares – pH = 7.1; diamonds – pH = 9.3; b – release kinetics of MeBT enclosed in PE containers: squares – pH = 7.0; diamonds – pH = 9.2.

The shapes of release curves is also remarkably differs from each other: the release of 8HQ is composed of the initial quite steep burst phase (Fig. 8a) followed by the very gradual saturation phase with almost plateau-like course of the curve. Moreover, this character of the release curve becomes more pronounced at the increase of pH of the release medium. On the contrary, the release of MeBT from PE containers is more gradual especially at the initial stage and is almost pH independent (Fig. 8b). These shapes of release dependencies become more understandable upon consideration of pH sensitivities of both containers matrices and the inhibitors enclosed within containers. Whereas MeBT as non-ionic substance is insensitive to the charge of containers matrix and independent of pH values in the surrounding medium, amphoteric character of 8HQ contributes to its interaction with the containers matrix and to the clearly expressed pH dependence of its release kinetics. In the neutral pH range, the water solubility of 8HQ [20, 21, 23, 24] is comparable with this of MeBT [25] but interaction with containers shell material (PUa or PE) at the interface with surrounding aqueous medium is in the case of 8HQ stronger causing its higher boundary solubility. As a result, the 8HQ loaded containers show faster (especially on the initial stage) release kinetics than PE containers with MeBT load. The discussed difference becomes more pronounced at the increase of pH from neutral to moderately alkaline value (compare Figs. 8a and 8b). This pH shift does not affect the non-ionic MeBT whereas the amphoteric 8HQ is more ionized

(deprotonated) in the alkaline range and, as a consequence, more soluble. Moreover, the release kinetics of 8HQ in this pH area could be additionally accelerated due to almost uncharged state of containers matrix and thus its less intensive interaction with the inhibitor load what is confirmed by the experiment.

3.3 Anticorrosive performance (on the basis of NSS tests data)

To evaluate the corrosion protection performance of coatings with containers based additives, numerous comparative NSS tests were carried out. Steel panels coated with conventional coatings, coatings without any ACPs (dummy) but directly doped by inhibitors and the same coatings with some percent of containers loaded with the same inhibitors were subjected to NSS tests of various duration. At the end of each test, the panels were withdrawn from NSS chamber, conditioned for at least 1 hour and scratched on the scribe. Then, the creepage extent on scribe to bare metal was measured in at least 15 points across the scribe and mean value was calculated.

The results of NSS-test for fatty acid modified alkyd resin coatings are presented in the figure 9. Whereas the conventional coating with 9.5 wt% ACP is completely failed after 328 h of test and demonstrated the well-expressed creepage and strong blistering (left panel, Fig. 9), the same coatings containing 2.5 wt% containers loaded with different corrosion inhibitors showed almost no signs of corrosion after 500 h of NSS-test (Fig. 9, middle left and middle right panels) and even after 1000 h (Fig. 9, right panel). Although scratched on the scribe, the last sample did not reveal any observable creepage and was almost free from blisters.

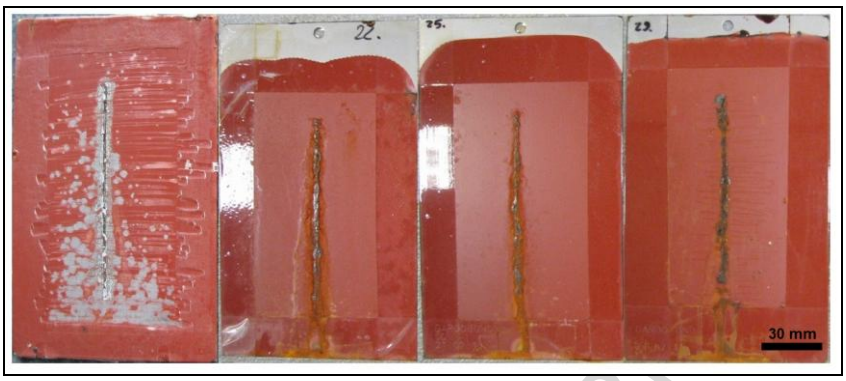

Figure 9. Results of the NSS tests for coatings on the basis of the fatty acid modified alkyd resin. From left to right: Conventional coating with 9.5 wt% ACPs after 328 h NSS; Dummy coating with 2.5 wt% PE containers loaded with BTA after 500 h NSS; Dummy coating with 2.5 wt% PUa containers loaded with MeBT after 500 h NSS; Dummy coating with 2.5 wt% PUa containers loaded with MeBT after 1000 h NSS. Scale bar corresponds to 30 mm.

The effect of the direct addition of corrosion inhibitor to the coating formulation is clearly seen in the Figure 10. Here, the corrosion protection performance of steel panels coated with conventional short oil modified alkyd resin coating containing 8 wt% of ACPs was compared with the protective performance of dummy coating (without any ACPs) directly doped with the corrosion inhibitor and the dummy coating containing 2.5 wt% containers loaded with the same corrosion inhibitor, respectively.

Figure 10. Results of the NSS tests for coatings on the basis of the short oil modified alkyd resin. From left to right: Conventional coating with 8 wt% ACPs after 500 h NSS; Dummy coating directly doped with 3 wt% MeBT after 500 h NSS; Dummy coating with 2.5 wt% PUa containers loaded with MeBT after 500 h NSS. Scale bar corresponds to 30 mm.

The strong negative effect of direct addition of the corrosion inhibitor in the free state is obvious – it caused a tremendous blistering over the whole area of the coated panel (Fig. 10, middle panel) after 500 h testing time. The panel coated with the conventional coating demonstrated quite low creepage on the scribe accompanying however by numerous large

blisters around the scribe (Fig. 10, left panel). The best protection against corrosion showed the panel coated by the dummy coating containing 2.5 wt% of inhibitor loaded containers – in this case no creepage on the scribe and only some small blisters over the panel area were observed (Fig.10, right panel). Noteworthy that the absolute concentration of the inhibitor in the coating matrix for the third panel was solely 1.5 wt% and therefore one half as much as the concentration of the same inhibitor added to the coating in the free state and more than 5 times lower than the concentration of ACPs in the conventional coating composition.

Another example undoubtedly confirming the advantages of anti-corrosive performance of the enclosed inhibitor over its free form added directly to the coating matrix is given in the Figure 11.

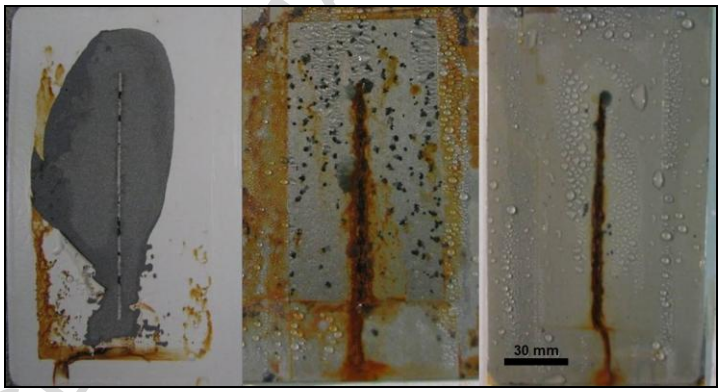

Figure 11. Results of the NSS tests for coatings on the basis of the waterborne styrene acrylic copolymer emulsions. From left to right: Conventional coating with 11.5 wt% ACPs after 140 h NSS; The same coating directly doped with 3 wt% MeBT after 300 h NSS; Dummy coating with 5 wt% PUa containers loaded with MeBT after 300 h NSS. Scale bar corresponds to 30 mm.

In this figure, the results of NSS test for steel panels coated with the waterborne styrene acrylic copolymer coatings are presented depending on the amount and form of the corrosion inhibitor incorporated in the coating matrix. Whereas the conventional styrene acrylic coating demonstrated a very high extent of creepage with the almost complete loss of adhesion to substrate already after 140 hours of testing (Fig.11, left), the same coating doped directly with 3 wt% of corrosion inhibitor could keep its integrity and adhesion over 300 hours of NSS test showed, however, a strong blistering on the panel surface (Fig. 11, middle). On the contrary, the dummy waterborne styrene acrylic coating (Fig. 11, right) with inhibitor loaded containers

showed after 300 hours of testing time neither observable creepage nor blistering. Taking into account the content of ACPs in the conventional styrene acrylic coating formulation, 11.5 wt%, especially in comparison with the total amount of the corrosion inhibitor enclosed in containers (3 wt%) one can see not only an absence of negative interaction effects for the enclosed inhibitor but also a significant enhancement of the total corrosion protection performance for the coatings with incorporated containers.

The physicochemical nature of the inhibitor enclosed in containers plays an important role in the protective efficiency of the coating in which these containers are embedded. As was shown above, short oil modified alkyd resin coatings with 2.5 wt % of PUa containers loaded with corrosion inhibitor MeBT demonstrated an outstanding protection effciency comparing with the conventional coatings of this type (Fig. 10). These coatings demonstrated only a slight blistering and almost no creepage after 500 hours of NSS test in contrast to the conventional coatings where strong blistering was observed. In spite of this improvement, the corresponding coatings are failed at the longer testing time especially against the background of the same coatings with 5 wt% of containers loaded with other corrosion inhibitor – 8HQ. Figure 12 shows the steel panels coated with short oil modified alkyd resin coatings containing 2.5 wt% of PUa containers with MeBT load and panels posessing the same coatings with 5 wt% of PUa containers loaded with 8HQ after 1000 hours of NSS test.

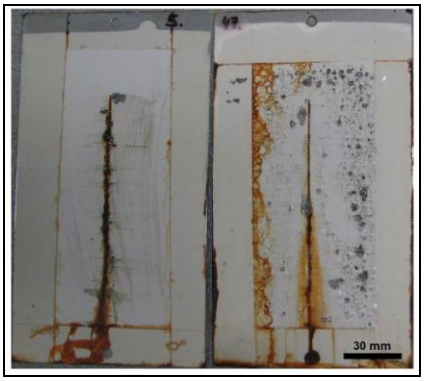

Figure 12. Effect of the physicochemical properties of the inhibitor loaded in containers on the corrosion resistance of coatings with incorporated containers. Coatings on the basis of short oil modified alkyd resin after 1000 hours of NSS test. Left – coating with 5 wt% PUa containers loaded with 8HQ; right – coating with 2.5 wt% PUa containers loaded with MeBT. Scale bar corresponds to 30 mm.

Unfortunately, the coatings with 2.5 wt% of PUa containers containing about 60 wt% MeBT were failed at this longer testing time: however, creepage on the scribe remained low also after 1000 hours of NSS hours, the blistering became quite strong especially on the numerous sites outside the scribe (Fig.12, right panel). On the contrary, the same type of coatings with 5 wt% of PUa containers with 8HQ load (slightly above 10 wt%) showed no blisters outside the scribe and some individual blisters close to it after the same duration of the NSS test (Fig.12, left panel). These finding are in the accordance with the results of EIS measurements for the short oil modified alkyd resin coatings which demonstrated no reduction in the barrier properties upon incorporation of inhibitor filled microcontainers (see Figure S3 in the section S3 of the Supporting Information (SI). The total amount of the incorporated inhibitor (8HQ) was in the second case approximately 3 times lower revealing much better corrosion resistance of the resulting coatings. This difference in the corrosion protection efficiency, especially in its long-term effect and sustainability, can be assigned to the differences in the chemical and physical properties of inhibitors used for the encapsulation in the containers. Indeed, in the neutral or slightly basic pH range typical for the scribe site during the NSS test, the 8HQ molecules exist predominantly in the deprotonated state $8Q^-$ and can form very stable complexes with iron cations (especially for the ferric ion Fe^{3+}). The structures of these complexes are depicted in the Figure 13 and present the chelate character of these compounds.

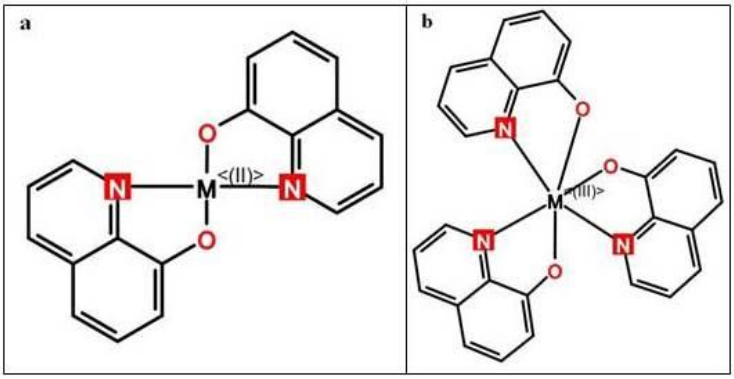

Figure 13. Schematic representation of the chemical structure of complexes formed by 8HQ with bi- and trivalent cations (like ferrous and ferric cations in the case of iron): a – structure of complex with bivalent cations; b – structure of complex with trivalent cations.

The corresponding logarithmic stability constants are high to very high and amount to15÷18 and even to 37 for $Fe(8Q)_2$ (Fig. 13a) and $Fe(8Q)_3$ (Fig. 13b), respectively [26]. The dense layer of these complexes covers the surface of steel panel on the scribe site and protects the bare metal from the further corrosive attacks. Moreover, this layer has also very low solubility in aqueous media – logarithmic solubility constant of $Fe(8Q)_3$ complex has for example the value of 43 to 44 [26]. On the other hand, the complexes of steel with MeBT with comparable stabilities only can be formed in strongly acidic conditions at which the surface of steel has a positive charge and the interaction of these positively charged sites with nucleophilic area in the molecules of MeBT and MeBT derivatives can provoke the formation of stabile complexes [27-29]. At the conditions of NSS testing, however, the stability of MeBT complexes with iron is essentially lower leading to the possible local excess of the inhibitor (remember its higher total concentration in containers in the case of MeBT) and its gradual leaching from the containers in spite of encapsulated form. Since this process is quite slow it becomes observable only at quite long duration of the NSS testing, as we can see in the comparison given in the Figure 12.

4. Conclusions

Novel corrosion protection additives based on inhibitor loaded polymeric micro- and nanocontainers prepared via emulsion route using interfacial polymerization processes present a valuable "green" alternative to conventional anticorrosive pigments. Amounts of latter typically ranging from 7.5 wt% to 11.5 wt% in conventional waterborne styrene acrylic copolymer and alkyd resin emulsions were successfully substituted by 3 to 4 times lower amounts of containers. The resulting anticorrosive coatings demonstrated strong increase of protective performance (up to several times better) comparing with the conventional coatings. This outstanding corrosion protection efficiency can be related to the specific properties and

structure of additives composing containers enabling corrosion triggered sustained consumption of encapsulated corrosion inhibitors.

Acknowledgments

This work was supported by the European G8 project G8MUREFU2-FP-377-0081 "Multiscale smart coatings with sustained anticorrosive action – smart coat". DS acknowledges ERC Consolidator grant ENERCAPSULE for financial support. DG is grateful for the financial support of the Federal Ministry of Economics and Energy (BMWi), Germany in the framework of "EXIST Transfer of Research" program (Project "SigmA" Nr. 03EFCBB028).

References

[1] R. Oppl, S.K. Simonsen, VOC emissions – new approaches for LEED, for ecolabels, for French regulations, Proceedings of Advances in Coatings Technology (ACT' 12) Conference, 9-11 October 2012, Sosnowiec, Poland, Paper Nr.31, 465-470.

[2] Council Directive 1999/13/EC of 11 March 1999 on the limitation of emissions of volatile organic compounds due to the use of organic solvents in certain activities and installations, Official J. of Eur. Comm. (1999) L85/1-L85/22.

[3] http://www.eastman.com/Literature_Center/N/N344.pdf, last successful access – 27th December 2015.

[4] http://www.eastman.com/Literature_Center/N/N322.pdf, last successful access – 27th December 2015.

[5] allnex.com/brochures/259, last successful access – 27th December 2015.

[6] http://www2.basf.us/corporate/tradeshows/acs/docs/ClosingTheGap-AnticorrosionCoatings.pdf, last successful access – 27th December 2015.

[7] S. González, I.C. Mirza Rosca, R.M. Souto, Investigation of the corrosion resistance characteristics of pigments in alkyd coatings on steel, Prog. Organic Coatings 43 (2001) 282-285.

[8] C.R. Hegedus, J.E. Sefko, C. Louis, and W. Chaigneau, Defoamers and Wetting Agents for Waterborne Alkyd Coatings, PCI 28 (2012) 42-50.

[9] S. Bender, N. Pietschmann, Das Unmögliche versuchen (in German), Farbe und Lack 6 (2014) 22-27.

[10] D.O. Grigoriev, M.F. Haase, N. Fandrich, A. Latnikova, D.G. Shchukin, Emulsion route in fabrication of micro and nanocontainers for biomimetic self-healing and self-protecting functional coatings, Bioinspir. Biomim. Nan. 1 (2012) 101-116.

[11] D. Grigoriev, D. Akcakayiran, M. Schenderlein, and D. Shchukin, Protective Organic Coatings with Anticorrosive and Other Feedback-Active Features: Micro- and Nanocontainers-Based Approach, Corrosion 70 (2014) 446-463.

[12] A. Latnikova, Polymeric capsules for self-healing anticorrosion coatings, PhD thesis, Potsdam University, Potsdam, Germany, 2012. Accessible online at the Institutional Repository of the University of Potsdam: http://opus.kobv.de/ubp/volltexte/2012/6043/

[13] A. Latnikova, D.O. Grigoriev, H. Möhwald, and D.G. Shchukin, Capsules Made of Cross-Linked Polymers and Liquid Core: Possible Morphologies and Their Estimation on the Basis of Hansen Solubility Parameters, J. Phys. Chem. C 116 (2012) 8181-8187.

[14] A. Latnikova, D. Grigoriev, H. Möhwald, D. Shchukin, Microgel containers for self-healing polymeric materials: morphology prediction and mechanism of formation, Polymer 2015, in press, DOI: 10.1016/j.polymer.2015.07.048

[15] ASTM B117, "Standard Practice for Operating Salt Spray (Fog) Apparatus" (West Conshohocken, PA: ASTM International, 2011), doi: 10.1520/B0117-11.

[16] S.D. Pandita, L. Wang, R.S. Mahendran, V.R. Machavaram, M.S. Irfan, D. Harris, G.F. Fernando, Simultaneous DSC-FTIR spectroscopy: Comparison of cross-linking kinetics of an epoxy/amine resin system, Thermochim. Acta 543 (2012) 9-17.

[17] B. Abismail, J.P. Canselier, A.M. Wilhelm, H. Delmas, C. Gourdon, Emulsification by ultrasound: drop size distribution and stability, Ultrason. Sonochem. 6 (1999) 75-83.

[18] C.M. Hansen, Hansen Solubility Parameters: A User's Handbook, second ed., CRC Press, Boca Raton, FL, 2007.

[19] I. Hofmeister, K. Landfester, and A. Taden, Controlled Formation of Polymer Nanocapsules with High Diffusion-Barrier Properties and Prediction of Encapsulation Efficiency, Angew. Chem. Int. Ed. 54 (2015) 327-330.

[20] A. Albert and A. Hampton, Ana1ogues of 8-Hydroxyquinoline having Additional Cyclic Nitrogen Atoms. Part II. Further Preparations, and Some Physico-chemical Properties, J. Chem. Soc. (1954) 505-513.

[21] S.M. Kaiser, Interactions of copper and hydrophobic ionogenic organic pollutants in biological membranes and their consequences for bioavailability and toxicity towards algae, PhD thesis, Swiss Federal Institute of Technology Zurich, Zurich, Switzerland, 2007. Accessible online at: http://library.eawag.ch/EAWAG-Publications/openaccess/Eawag_04842.pdf

[22] J.J. Ellington, Octanol/Water Partition Coefficients and Water Solubilities of Phthalate Esters, J. Chem. Eng. Data 44 (1999) 1414-1418.

[23] T. Robinson, Equilibrium speciation of select lanthanides in the presence of acidic ligands in homo- and heterogeneous solutions, PhD thesis, University of Nevada, Las Vegas, USA, 2011.

[24] M.F. Haase, D. Grigoriev, H. Moehwald, B. Tiersch, and D.G. Shchukin, Encapsulation of Amphoteric Substances in a pH-Sensitive Pickering Emulsion, J. Phys. Chem. C 114 (2010) 17304-17310.

[25] N-Cyclohexylbenzothiazol-2-sulphenamide, Summary risk assessment report, Final report, May 2008, Germany. Accessible online at: http://echa.europa.eu/documents/10162/48e99dc2-8d09-47e5-b167-61e8d2b13fd1

[26] J. Stary, Yu.A. Zolotov and O.M. Petrukhin, Critical Evaluation of Equilibrium Constants involving 8-Hydroxyquinoline and its Metal Chelates, IUPAC Chemical Data Series, No. 24, Pergamon Press, Oxford, 1979.

[27] A.M. A1-Mayouf, A.A. A1-Suhybani, A.K. A1-Ameery, Corrosion inhibition of 304SS in sulfuric acid solutions by 2-methyl benzoazole derivatives, Desalination 116 (1998) 25-33.

[28] Z. Moradi, M.M. Attar, An investigation on the inhibitory action of benzazole derivativesas a consequence of sulfur atom induction, Appl. Surf. Sci. 317 (2014) 657-665.

[29] K. Parameswari, S. Chitra, A. Selvaraj, S. Brindha and M. Menaga, Investigation of Benzothiazole Derivatives as Corrosion Inhibitors for Mild Steel, Port. Electrochim. Acta 30 (2012) 89-98.

Figure captions

Figure 1. A: i – Preparation of initial emulsion with the dispersed phase containing corrosion inhibitor and first reactant participating in the interfacial polyaddition reaction, emulsion stabilizer/surfactant is dissolved in the dispersion medium; ii – Addition of bulk-soluble second reactant for the interfacial polyaddition in the pre-formed emulsion and start of polyaddition reaction. Inset – interfacial polyaddition process on the boundary of emulsion droplets; iii – Completion of micro- or nanocontainers formation with core/shell or compact morphology. B: i – Preparation of an initial emulsion with the dispersed phase containing corrosion inhibitor and all reactants needed for the in-situ polyaddition, emulsion stabilizer/surfactant is dissolved in the dispersion medium; ii – Addition of bulk-soluble initiator for the polyaddition reaction in the pre-formed emulsion and start of in-situ polyaddition. Inset – in-situ polyaddition reaction in the bulk of each emulsion droplet; iii – as in A iii.

Figure 2. Schematic illustration of the test panels preparation process: I – degreasing; II – incorporation of containers in an appropriate coating formulation; III – application by spraying; IV – curing.

Figure 3. Gradual increase of the isocyanate conversion degree in the course of PUa containers formation: 1 – initial "oil" phase containing unreacted isocyanate prepolymers; 2 – premature containers after first 30 minutes of synthesis; 3 – ready containers.

Figure 4. a – Results of several subsequent Zeta-potential measurements obtained at pH 7 for aqueous suspension of PUa containers loaded with the corrosion inhibitor 8HQ; b – Zeta-potential measured for aqueous suspension of MeBT filled PE containers at pH = 6.7.

Figure 5. Size distributions of PUa and PE containers (zeta average) determined by DLS for their aqueous suspension in neutral pH range: a – PUa containers loaded with the corrosion inhibitor 8HQ using DEPh as an auxiliary solvent in the step of the initial emulsion

preparation; b – as in a. but with MeTHF as an auxiliary solvent; c – PUa containers loaded with the liquid corrosion inhibitor MeBT; d – PE containers loaded with the corrosion inhibitor BTA; e – PE containers loaded with the liquid corrosion inhibitor MeBT.

Figure 6. SEM and TSEM observations of inhibitor loaded PUa and PE containers: a – PUa containers loaded with the corrosion inhibitor 8HQ using DEPh as an auxiliary solvent; b – PUa containers loaded with the corrosion inhibitor 8HQ using MeTHF as an auxiliary solvent; c – PUa containers loaded with the liquid corrosion inhibitor MeBT; d and e – PE containers loaded with the corrosion inhibitor BTA in SEM and TSEM mode, respectively; f – PE containers loaded with the liquid corrosion inhibitor MeBT. Scale bars correspond to 2 µm, 1µm, 300 nm and 100 nm for pictures a and b; c; d and e; and f, respectively.

Figure 7. a – TGA curve of PUa containers loaded with the corrosion inhibitor 8HQ (2) compared with the TGA of the pure substance (1); b – TGA curve of PUa containers loaded with the liquid corrosion inhibitor MeBT (2) compared with the TGA of the pure substance (1). Vertical straight lines correspond to the boiling points of pure 8HQ and MeBT.

Figure 8. a – release kinetics of 8HQ enclosed in PUa containers: squares – pH = 7.1; diamonds – pH = 9.3; b – release kinetics of MeBT enclosed in PE containers: squares – pH = 7.0; diamonds – pH = 9.2.

Figure 9. Results of the NSS tests for coatings on the basis of the fatty acid modified alkyd resin. From left to right: Conventional coating with 9.5 wt% ACPs after 328 h NSS; Dummy coating with 2.5 wt% PE containers loaded with BTA after 500 h NSS; Dummy coating with 2.5 wt% PUa containers loaded with MeBT after 500 h NSS; Dummy coating with 2.5 wt% PUa containers loaded with MeBT after 1000 h NSS. Scale bar corresponds to 30 mm.

Figure 10. Results of the NSS tests for coatings on the basis of the short oil modified alkyd resin. From left to right: Conventional coating with 8 wt% ACPs after 500 h NSS; Dummy coating directly doped with 3 wt% MeBT after 500 h NSS; Dummy coating with 2.5 wt% PUa containers loaded with MeBT after 500 h NSS. Scale bar corresponds to 30 mm.

Figure 11. Results of the NSS tests for coatings on the basis of the waterborne styrene acrylic copolymer emulsions. From left to right: Conventional coating with 11.5 wt% ACPs after 140 h NSS; The same coating directly doped with 3 wt% MeBT after 300 h NSS; Dummy coating with 5 wt% PUa containers loaded with MeBT after 300 h NSS. Scale bar corresponds to 30 mm.

Figure 12. Effect of the physicochemical properties of the inhibitor loaded in containers on the corrosion resistance of coatings with incorporated containers. Coatings on the basis of short oil modified alkyd resin after 1000 hours of NSS test. Left – coating with 5 wt% PUa containers loaded with 8HQ; right – coating with 2.5 wt% PUa containers loaded with MeBT. Scale bar corresponds to 30 mm.

Figure 13. Schematic representation of the chemical structure of complexes formed by 8HQ with bi- and trivalent cations (like ferrous and ferric cations in the case of iron): a – structure of complex with bivalent cations; b – structure of complex with trivalent cations.

Highlights

- Green corrosion inhbitors were enclosed in the polymeric micro- and nanocontainers
- Containers made of polyurea and (poly)epoxy resin were prepared by emulsion route
- Containers morphology is determined by the polymer/load polarity difference
- Containers embedded in usual waterborne coatings improve their corrosion resistance
- Replacement of common pigments by containers enhance eco-friendliness of coatings